IEEE Access
Multidisciplinary | Rapid Review | Open Access Journal

Received October 10, 2019, accepted November 9, 2019, date of publication November 14, 2019,
date of current version November 26, 2019.

Digital Object Identifier 10.1109/ACCESS.2019.2953496

A Novel Approach of Hybrid Trigonometric Bézier Curve to the Modeling of Symmetric Revolutionary Curves and Symmetric Rotation Surfaces

SAMIA BIBI[1], MUHAMMAD ABBAS[1], MD YUSHALIFY MISRO[2], AND GANG HU[3]
[1]Department of Mathematics, University of Sargodha, Sargodha 40100, Pakistan
[2]School of Mathematical Sciences, Universiti Sains Malaysia, Penang 10800, Malaysia
[3]Department of Applied Mathematics, Xi'an University of Technology, Xi'an 710054, China

Corresponding authors: Muhammad Abbas (muhammad.abbas@uos.edu.pk) and Md Yushalify Misro (yushalify@usm.my)

This work was supported by the Universiti Sains Malaysia under Grant 304/PMATHS/6315223.

ABSTRACT The modeling of Bézier curves and surfaces with their shape parameters is the most popular area of research in computer aided geometric design/computer aided manufacturing (CAGD/CAM) due to their geometric characteristics. In this paper, we propose an important idea to tackle the problem in construction of some engineering symmetric revolutionary curves and symmetric rotation surfaces by using the generalized hybrid trigonometric Bézier (or GHT-Bézier, for short) curve. The shape of the curves and surfaces can be modified by the alteration of shape parameters. The free-form complex curves using GHT-Bézier curves with constraints of parametric continuity are constructed. Finally, by using the GHT-Bézier curves with their continuity conditions and symmetric formulas, we construct different types of symmetric figures, symmetric revolutionary curves and symmetric rotation surfaces in $\mathbb{R}^2$ and $\mathbb{R}^3$ to show the efficiency of modeling. These symmetric examples show that the proposed method is time saving, effective and efficient in construction of complex engineering symmetric curves and surfaces.

INDEX TERMS GHT-Bernstein basis functions, GHT-Bézier curves, parametric continuity, shape parameters, symmetric revolutionary curves, symmetric rotation surfaces.

I. INTRODUCTION

In mathematics, manufacturing and engineering field, a solid of revolution is a surface (solid) which is obtained by revolving a plane curve (area). Revolutionary axis is an option where the solid revolution curve can be easily rotated. Like this, symmetric curves and symmetric surfaces are that set of data points which can show the mirror image of the same figure around that axis in the left side. These curves and surfaces can be represented in CAD/CAM field in terms of two and three tuples. Since traditional Bézier curves can be obtained by control points and Bernstein basis functions. After creating Bézier curves and surfaces we can construct different shapes by using parametric and geometric continuities which fulfill our design requirements. Since shape designing is a time consuming process and usually we cannot execute our required design in one step even though by using continuity conditions. Especially, when we are going to established some complex symmetric revolutionary curves and symmetric rotation surfaces by the help of Bézier curves. In order to overcome this cumbersome problem we define two different functions to construct these curves and surfaces in two and three tuples. Since trigonometric Bézier curve with the shape parameters is more continuous as compared to polynomial Bézier curve. By the variation of shape parameters we can modify the shape according to our own choice.

Recently, many scholars got more attention to the trigonometric Bézier curves. Xikum [1] constructed Bernstein-Bézier curve with the shape parameters, but that curve was not symmetric curve. Yan and Liang [2] defined generalized Bézier-like curve. They extended the generalized Bézier-like curve to tensor product surface and further they approach to the triangular surfaces. Li *et al.* [4] presented the modeling of revolutionary surfaces based on the stream curves. Which are also presented by the integral form of tangent vectors. Liu *et al.* [5] also presented the cubic trigonometric polynomial B-spline curve and surfaces modeling. They presented the various curves and surfaces modeling by the

The associate editor coordinating the review of this manuscript and approving it for publication was Shunfeng Cheng.

variation of shape parameters. Li [6] defined α-Bézier curves of degree n with shape parameter α by extending the definition of Bézier curve and also presented the properties and applications of α-Bézier curves. Wen-Tao and Guo-Zhao [7] defined Bézier-like curves having the shape parameter by an integral approach. Hu *et al.* [8] constructed a Developable Bézier-like surfaces with their properties and presented different type of complex surfaces modeling by using C^2 and G^2 continuity conditions. Han *et al.* [9] constructed a cubic trigonometric Bézier curve with two shape parameters and also made the ellipse by using it.

Hu *et al.* [11] presented a new method for the construction of shape adjustable generalized Bézier rotation surfaces with the multiple shape parameters. They form an explicit function by using transfinite vectored rational interpolation for the construction of an algorithm to form rotation surfaces. Hu *et al.* [12] presented a novel extension for the modeling of Bézier curves and surfaces and their applications in manufacturing and engineering field. Hu *et al.* [13] presented the modeling of free form complex curves by using parametric and geometric continuities. They also used the multiple shape parameters to modify and beautify the complex curves according to requirement. Qin *et al.* [15] constructed a class of new polynomial basis functions with $(n-1)$ local shape parameters, which is an extension to the classical Bernstein basis functions of degree n. The properties of these basis functions and their C^2 and G^2 continuity conditions are also presented with the best approximation.

Cubic and quartic trigonometric Bézier curves with their shape parameters were presented in [16], [19]. The properties of these Bézier curves and effect of the shape parameter is also studied. Special rotation surfaces with their significant improvement have been studied in [4]. But it has many drawbacks due to required symmetrical shape adjustability. In [20], Qin and Hu constructed the PH-Spline Bézier curves and presented their properties, edge and angle of its control polygon. Bashir *et al.* [21] presented the rational quadratic trigonometric Bézier curve with two shape parameters. They also presented the conic section and other curves with their applications. Han [22] described the piecewise quadratic trigonometric polynomial curves, presented its C^2 continuity conditions and showed that the quadratic trigonometric polynomial curve has a closer control polygon as compared to the control polygon of quadratic B-Spline curve. Misro *et al.* [25], [26] constructed C-shape and S-shape transition curves and maximum speed estimation on highway design by using cubic and quintic trigonometric Bézier curves respectively. G^2 Hermite conditions and numerical examples are also discussed in [25].

Yan [27] presented a particular family of Bézier curves with three different shape parameters which are also known as adjustable Bézier curves. These curves have same shape and structure like quartic Bézier curve. Hu *et al.* [28] constructed the designing of local controlled by using control planes and developable H-Bézier surfaces and also presented the C^2 continuity and G^2 beta continuity between the developable generalized H-Bézier surface and constructed different modeling examples. Sharma [29] constructed quartic trigonometric Bézier (QTB) curve with two different shape parameters, the properties of QTB curve with various modeling and shape control of the curve is also discussed. In [30], a new parameterized surface termed as SQ-Coons surface is proposed according to the build mode of coons patch. This result improves the design and scheme adjustment efficiency in the conceptual design stage.

In the study from Fu *et al.* [31], the influence of various eddy viscosity turbulence models on the CFD simulations of a particular racing car typing is discussed. They also pointed out that the shape of some specific surfaces (i.e., backlight-decklid junction, spoiler base, roof rails, shark fin) would affect the result of CFD simulation. Chowdhuary *et al.* [32] built a bio inspired CAD car model to take advantage of the boxfish in water due to its streamline features. The shape of this model in unified and integral and its characteristic lines consist of the intersection of several subsurfaces. Hsu *et al.* [33], proposed a new boundary representation method of the CAD model, which is more suitable for mesh generation in CFD preprocessing. From the prediction of Kumar and Sarkar [34], the similar feature descriptions extracted from historical models could be used to predict the vehicle design trend. In their further research [35], a series of related styling features was integrated into a style-holon to describe the internal evolution trend of brand characteristics. Guo *et al.* [36] proposed a novel algorithm to automatically transform the CAD model into high quality mesh according to its shape features line. Xiong *et al.* [37] proposed that designers influence users psychological feelings through the representation of a product's conceptual features.

Pei *et al.* [38] replaced the blending function in the second type of Coons patch with a second order trigonometric blending function, a blending function with the shape parameter λ and a RBF-Hermit function to make the patch shape modifiable. Shen and Wang [39] proposed a new transformation algorithm to define the C-Bézier curve with one shape parameter introduced as a seperated form including a Bézier part and a trigonometric part in order to represent some regular curves such as a cycloid or traditional Bézier curve by the C-Bézier curve. Aljure *et al.* [40] found a comparison between the large eddy simulation model and the wall modeled large eddy simulation and a realistic generic car body CAD model according to the styling of the Audi *A*4 and the BMW 3 series was adopted. Since the shape adjustability is the most prominent characteristic of H-Bézier model in curves and surfaces modeling and means that the research in it is practical and theoretical values given in [41], [42]. In [43], [44], the adjustment of the shape according to the Bézier model is discussed.

II. A FAMILY OF GHT-BÉZIER CURVES

The definition and general properties of GHT-Bézier curve are defined as follows.

A. THE GHT-BERNSTEIN BASIS FUNCTIONS

Definition 1: Let we consider the shape parameters $\mu, \alpha, \omega \in [-1, 1]$ and $\lambda \in [-1.5, 0.5]$, the following function in terms of variable t,

$$\begin{cases} S_{0,2}(t) = (1 - sin(\frac{\pi}{2}t)[(1 - \mu sin(\frac{\pi}{2}t))e^{\omega t} \\ \qquad + \lambda(1 - cos(\frac{\pi}{2}t))], \\ S_{1,2}(t) = 1 - S_{0,2}(t) - S_{2,2}(t), \\ S_{2,2}(t) = (1 - cos(\frac{\pi}{2}t)[(1 - \alpha cos(\frac{\pi}{2}t))e^{(1-\omega)t} \\ \qquad - \lambda(1 - sin(\frac{\pi}{2}t))], \end{cases} \tag{1}$$

is called the hybrid trigonometric Bernstein-like basis function of degree 2. For any integer n, where $(n \geq 3)$ the function $S_{i,n}(t)$ $(i = 0, 1, 2, \ldots, n)$, defined by the following recursive formula,

$$S_{i,n}(t) = (1 - t)S_{i,n-1}(t) + tS_{i-1,n-1}(t), \tag{2}$$

is called GHT-Bernstein basis functions of degree n. Especially for the case, when $i = -1$ or $i > n$ the function $S_{i,n}(t) = 0$.

Figure 1 shows the graphical representation of GHT-Bernstein basis functions of multiple degrees by variation of shape parameters.

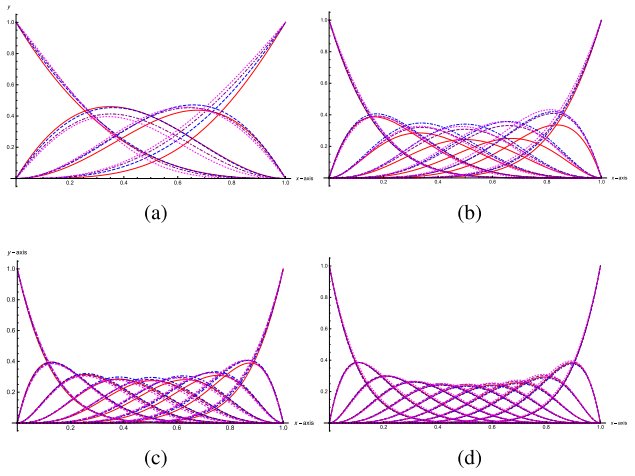

FIGURE 1. **GHT-Bernstein basis functions with shape parameters μ = (0.5, 0, −0.5, −1), α = (0.5, 0, −0.5, −1), ω = (0.5, 0, −0.5, −1), λ = (0.5, 0, −0.5, −1) of different degrees. (a): n = 3. (b): n = 6. (c): n = 8. (d): n = 10.**

Theorem 1: The GHT-Bernstein basis functions have the following properties:

1) **Non-negativity**: For any $\mu, \alpha, \omega \in [-1, 1]$, and $\lambda \in [-1.5, 0.5]$, the function $S_{i,n}(t) \geq 0$ where $(i = 0, 1, 2, \ldots, n)$.
2) **Partition of unity**:

$$\sum_{i=0}^{n} S_{i,n}(t) = 1.$$

3) **Symmetry**: When we keep all shape parameters equal such as, $\mu = \omega = \alpha = \lambda$, then $S_{i,n}(t)(i = 0, 1, 2, \ldots, n)$ are symmetric i.e

$$S_{i,n}(t, \mu, \alpha, \omega, \lambda) = S_{n-i,n}(1 - t, \mu, \alpha, \omega, \lambda).$$

4) **Terminal Properties**: The GHT-Bernstein basis functions have the following properties at end points.

$$\begin{cases} S_{i,n}(0) = 1, & i = 0. \\ S_{i,n}(0) = 0, & i = 1, 2, 3, \ldots, n. \\ S_{n,n}(1) = 1, & i = n. \\ S_{i,n}(1) = 0, & i = 0, 1, 2, 3, \ldots, n - 1. \end{cases} \tag{3}$$

and the first derivative of these functions at their end points are:

$$\begin{cases} S'_{i,n}(0) = \frac{1}{2}[-\pi(1+\mu) - 2((n-2) - \omega)], & i = 0. \\ S'_{i,n}(0) = (n-2) + \frac{1}{2}\pi(1+\mu) - \omega, & i = 1. \\ S'_{i,n}(0) = 0, & i = 2, 3, 4, \ldots, n. \\ S'_{i,n}(1) = 0, & i = 0, 1, 2, 3, \ldots, n-2. \\ S'_{i,n}(1) = \frac{1}{2}[-\pi(1+\alpha) - 2((n-2) - \omega)], \\ \qquad\qquad i = n - 1. \\ S'_{i,n}(1) = (n-2) + \frac{1}{2}\pi(1+\alpha) - \omega, & i = n. \end{cases} \tag{4}$$

Similarly, the second derivative of these functions at the end points are:
when n is even

$$\begin{cases} S''_{i,n}(0) = \frac{\pi^2}{4}(\lambda + 2\mu) - \pi(1+\mu)(-(n-2)+\omega) \\ \qquad + \omega^2 - (2n-4)\omega + k(2n-4) - (n-2), \\ \qquad\qquad i = 0, k \in W \\ S''_{i,n}(1) = 0, \quad i = 0 \\ S''_{i,n}(0) = 0, \quad i = n \\ S''_{i,n}(1) = \frac{\pi^2}{4}(2\alpha - \lambda) - \pi(1+\alpha)(-(n-2)+\omega) \\ \qquad - (2n-4)\omega + k\,(2n-4) - (n-2), \\ \qquad\qquad i = n, k \in W \\ S''_{i,n}(1) = \frac{\pi^2}{4}e^{\omega}(\mu - 1) + (1-\alpha)\pi\omega - \omega^2 + \omega^2 \\ \qquad - \frac{1}{2}\pi^2\alpha, \quad i = 1, n = 2 \\ S''_{i,n}(0) = \frac{\pi^2}{4}(e^{\omega}(\alpha - 1) - 2\mu) + \pi(1+\mu)(\omega \\ \qquad - 4k) - \omega^2 + 8k\omega - 4(2k-1)k, \\ \qquad n = 2, 4, 6, \ldots i = 1, k \in W \\ S''_{i,n}(1) = 0, \quad i = 1, n = 4, 6, 8, \ldots \end{cases} \tag{5}$$

when n is odd.

$$\begin{cases} S''_{i,n}(0) = \frac{\pi^2}{4}(\lambda + 2\mu) - \pi(1+\mu)(-(n-2) \\ \quad + \omega) + \omega^2 - (2n-4)\omega + k(2n-4), \\ \quad i = 0, k \in W \\ S''_{i,n}(1) = 0, \quad i = 0 \\ S''_{i,n}(0) = 0, \quad i = n \\ S''_{i,n}(1) = \frac{\pi^2}{4}(2\alpha - \lambda) - \pi(1+\alpha)(-(n-2) \\ \quad + \omega) + \omega^2 - (2n-4)\omega + k(2n-4), \\ \quad i = n, k \in W \\ S''_{i,n}(1) = \pi + \pi\alpha + \frac{\pi^2}{4}(\lambda - e^{\omega}(\mu - 1) - 2\omega, \\ \quad i = 1, n = 3 \\ S''_{i,n}(0) = \frac{\pi^2}{4}(e^{\omega}(\alpha -) - 2\mu) + (12 + 8r)(\omega \\ \quad - k) + \pi(1+\mu)(\omega - (4k+2)) - \omega^2, \\ \quad i = 1, r, k \in W, n = 3, 5, 7, \ldots \\ S''_{i,n}(1) = 0, \quad i = 1, n = 5, 7, 9, \ldots. \end{cases} \tag{6}$$

and

$$\begin{cases} S''_{i,n}(0) = \frac{1}{4}[4(n-2)\pi(1+\mu) - \pi^2(e^{\omega}(\alpha - 1) \\ \quad + \lambda) - 8(n-2)\omega + 8(V_r + r + 1)], r \in W, \\ \quad i = 2, V_r = V_{r-1} + r, V_{-1} = V_0 = 0, \\ \quad n = 3, 4, \ldots, \\ S''_{i,n}(0) = 0, \quad i = 3, 4, 5, 6, \ldots, n-1 \\ S''_{i,n}(1) = \frac{1}{4}\pi^2(-2\alpha + e^{\omega}\mu - 1) + \pi(\omega - 2(n \\ \quad - 2))(1+\alpha) - (\omega^2 - 4(n-2)\omega + 4(V_r \\ \quad + r + 1), V_r = V_{r-1} + r, V_{-1} = V_0 = 0, \\ \quad i = n-1, n \geq 3, r = 0, 1, 2, 3, 4, \ldots \\ S''_{i,n}(1) = \frac{1}{4}[(4(n-2)\pi(1+\alpha) + 8(V_r + r \\ \quad + 1) + \pi^2(\lambda - e^{\omega}(-1+\mu)) - 8(n-2)\omega], \\ \quad i = n-2, V_r = V_{r-1} + r, V_{-1} = V_0 = 0, \\ \quad n \geq 4, r \in W \\ S''_{i,n}(1) = 0, \quad n \geq 5, \ i = n-3, n-4, n-5, \ldots \end{cases} \tag{7}$$

Proof: It is obvious to obtain these result from Definition 1.

B. CONSTRUCTION OF GHT-BÉZIER CURVES WITH SHAPE PARAMETERS

Definition 2: For the given control points $P_i (i = 0, 1, 2, 3, \ldots, n)$, the curve

$$\{\Pi_t\} : H(t; \mu, \alpha, \omega, \lambda) = \sum_{i=0}^{n} P_i S_{i,n}(t), \quad 0 \leq t \leq 1 \tag{8}$$

is called GHT-Bézier curve. Where $S_{i,n}(t)$ are called GHT-Bernstein basis functions and μ, α, ω, λ are the shape parameters.

Theorem 2: The GHT-Bézier curves have the following properties:

1) **Shape adjustable property:** Since the classical Bézier curve is always fixed inside the control polygon and we cannot alter it without changing the control points. Because it do not possess the shape parameters. But GHT-Bézier curve having four different shape parameters. So, by fixing the control polygon, we can adjust the shape of the curve only by varying the shape parameters.
2) **Terminal properties:** For the given four shape parameters $\mu, \alpha, \omega \in [-1, 1]$ and $\lambda \in [-1.5, 0.5]$, we have the following terminal properties of the curve.

$$\begin{cases} H(0) = P_0, \\ H(1) = P_n, \\ H'(0) = \frac{1}{2}(2(n-2) + \pi(1+\mu) - 2\omega)(P_1 - P_0), \\ H'(1) = \frac{1}{2}(2(n-2) + \pi(1+\alpha) - 2\omega)(P_n \\ \quad - P_{n-1}), \\ H''(0) = \frac{1}{4}[\pi^2(\lambda + 2\mu) - 4\pi(1+\mu)((n-2) - \omega) \\ \quad + 4(\omega^2 - 2(n-2) + 12))P_0 + [\pi^2(e^{\omega} \\ \quad (\alpha - 1) - 2\mu + 4\pi(1+\mu)(\omega - 2(n-2)) \\ \quad - 4(\omega^2 - 4(n-2) + 4(U_z + z + 1))] P_1 \\ \quad + \pi^2(e^{\omega}(\alpha - 1) + \lambda) - 4k\pi(1+\mu) \\ \quad + 8r\omega + 8(V_r + r + 1)] P_2, \ U_k = U_{k-1} \\ \quad + k, \ V_r = V_{r-1} + r, \ U_0 = 0, \quad V_1 = 0, \\ \quad V_{-1} = 0, \quad r \in Z, \ k \in W, \\ H''(1) = \frac{1}{4}[4(U_k + k + 1)\pi(1+\alpha) + \pi^2(e^{\omega} \\ \quad (1-\mu)) - 8r\omega + 8(V_r + r + 1)] P_{n-2} \\ \quad + [\pi^2(-2\alpha + e^{\omega}(\mu + 1)) + 4\pi(1+\alpha)(\omega \\ \quad - (2n-4)) - 4(\omega^2 - (4n-8)\omega + (U_k \\ \quad + k + 1))]P_{n-1} + [\pi^2(2\alpha - \lambda) - 4\pi(1 \\ \quad + \alpha)(\omega - (n-3)) + 4(\omega^2 + (2n-4) \\ \quad \omega + 2(U_z + z + 1))]P_n, \ U_k = U_{k-1} + k, \\ \quad V_r = V_{r-1} + r, \ U_0 = 0, \ V_1 = 0, \ V_{-1} = 0, \\ \quad z \in Z, r \in Z, k \in W. \end{cases} \tag{9}$$

3) **Symmetry:** When we have $\mu = \alpha = \omega = \lambda$, the control points of this curve, $P_0, P_1, P_2, \ldots, P_{n-1}, P_n$ and $P_n, P_{n-1}, P_{n-2}, \ldots, P_1, P_0$ define the same GHT-Bézier curve having symmetric influence, such as:

$$\begin{aligned} &H(t; \mu, \alpha, \omega, \lambda, P_0, P_1, P_2, \ldots, P_{n-1}, P_n) \\ &= H(1-t; \lambda, \omega, \alpha, \mu, P_n, P_{n-1}, P_{n-2}, \ldots, P_1, P_0). \end{aligned} \tag{10}$$

4) **Convex hull property:** Since the above mentioned GHT-Bernstein basis functions have two properties, partition of unity and non-negativity, which infer that the GHT-Bézier curve with control points $P_0, P_1, P_2, \ldots, P_n$, must lie inside the control polygon.
5) **Geometric invariance:** The shape of GHT-Bézier curve never depends upon the coordinate axis, which means that this curve satisfies the following two equations:

$$\begin{aligned} &H(t;\mu,\alpha,\omega,\lambda;P_0+\widetilde{M},P_1+\widetilde{M},P_2+\widetilde{M},\ldots,P_n \\ &\quad+\widetilde{M})=H(t;\mu,\alpha,\omega,\lambda;P_0,P_1,P_2,\ldots,P_n)+\widetilde{M}, \\ &\quad H(t;\mu,\alpha,\omega,\lambda;WP_0,WP_1,WP_2,\ldots,WP_n) \\ &\quad=WH(t;\mu,\alpha,\omega,\lambda;P_0,P_1,P_2,\ldots,P_n), \end{aligned} \tag{11}$$

where $\widetilde{M}$ is an arbitrary vector in $\mathbb{R}^2$ or $\mathbb{R}^3$, W is an arbitrary $m \times m$ matrix for $m = 2, 3$.

Proof: It is obvious to obtain these result from Definition 2.

C. INFLUENCE OF SHAPE PARAMETER ON GHT-BÉZIER CURVES

The basis functions defined by Equation (2) possess four different shape parameters, by altering the value of these shape parameters, we can see the variation on the GHT-Bézier curves in Figure 2.

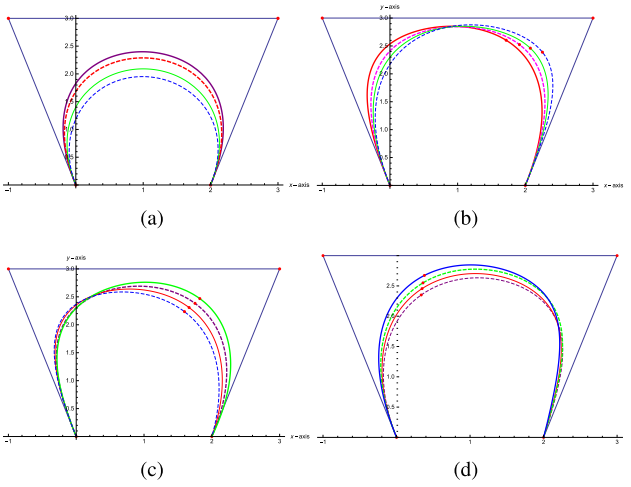

FIGURE 2. **Cubic Hybrid Trigonometric Bézier curves by the variation of shape parameters. (a): $\alpha = \lambda = \omega = 0$, $\mu = -0.6, -0.1, 0.5, 0.8$. (b): $\alpha = \mu = 1$, $\omega = -1$, $\lambda = -1.5, -1, -0.1, 0.5$. (c): $\omega = 0$, $\lambda = 1$, $\mu = \alpha = 1, 0.9, 0.83, 0.75$. (d): $\mu = \alpha = 1$, $\lambda = -1.5$, $\omega = 0, 0.5, -0.5, -1.34$.**

Consider a cubic hybrid trigonometric Bézier curve $P(t;\mu,\alpha,\omega,\lambda) = \sum_{i=0}^{3} P_i S_{i,3}(t)$ with four control points $P_0 = (0,0)$, $P_1 = (-1,3)$, $P_2 = (3,3)$ and $P_3 = (2,0)$. Figure 2(a) shows the smooth behavior of different curves by varying the shape parameters. Such as, when we keep the shape parameter $\alpha = \lambda = \omega = 0$ fixed and increase the value of $\mu = -0.6, -0.1, 0.5$ and 0.8 then the curves move towards the control polygon. Figure 2(b) also depicts the behavior of cubic curve by the variation of shape parameters. Here the given curve is generated by keeping the shape parameters $\alpha = \mu = 1$ and $\omega = -1$ fixed and by altering the values of $\lambda = -1.5, -1, -0.1, 0.5$. This curve shows a beautiful influence on both left and right side from the center of the curve. Figure 2(c) shows the behavior of the curve when we fix the values of the shape parameters $\omega = 0$ and $\lambda = 1$ and gives the simultaneous variation to the parameter $\mu = \alpha = 1, 0.9, 0.83, 0.75$. Here the curves show unique behavior, as we gradually decrease the value of the shape parameters the curves move towards the control polygon rather than moving away from the control net. Figure 2(d) also shows the influence on the curves by the variation of shape parameters. In this Figure, we again fix some shape parameters and vary few of them to check the behavior of the curve. We keep $\mu = \alpha = 1$ and $\lambda = -1.5$ fixed and give variations to the parameter $\omega = 0, 0.5, -0.5, -1.34$. The blue solid line is obtained by the minimum value of λ then by gradually decreasing these values the curves are moving farther away from the control net.

D. PARAMETRIC CONTINUITY CONSTRAINTS FOR GHT-BÉZIER CURVES

In CAGD and manufacturing system, we can obtain our required shape by adjusting the shape parameters of the curve. But various kinds of complex curves are difficult to be constructed by a single curve even though by adjusting the shape parameters. Therefore, continuity conditions are used to join multiple curves to obtain the required shape.

Consider two adjacent GHT-Bézier curves which are defined as:

$$\begin{cases} H_1(t;\mu_1,\alpha_1,\omega_1,\lambda_1) \\ \quad=\displaystyle\sum_{i=0}^{n} P_i S_{i,n}(t), \qquad 0 \le t \le 1, n \ge 3, \\ H_2(t;\mu_2,\alpha_2,\omega_2,\lambda_2) \\ \quad=\displaystyle\sum_{j=0}^{m} Q_j S_{j,m}(t), \qquad 0 \le t \le 1, m \ge 3, \end{cases} \tag{12}$$

where $S_{i,n}(t)$ and $S_{j,m}(t)$ are GHT-Bernstein basis functions of degree n and m, respectively. The $\mu_1, \alpha_1, \omega_1, \lambda_1$, $P_i (i = 0, 1, 2, 3, \ldots, n)$ and $\mu_2, \alpha_2, \omega_2, \lambda_2$, $Q_j (j = 0, 1, 2, 3, \ldots, m)$ are the shape parameters and control points of these two adjacent GHT-Bézier curves, respectively.

Theorem 3: Given two GHT-Bézier curves of same degrees

$$H_1(t;\mu_1,\alpha_1,\omega_1,\lambda_1) = \sum_{i=0}^{n} P_i S_{i,n}(t),$$

and

$$H_2(t;\mu_2,\alpha_2,\omega_2,\lambda_2) = \sum_{i=0}^{m} Q_j S_{j,m}(t),$$

the necessary and sufficient conditions for C^2 continuity at the joint points are given by

1) For C^0 continuity

$$Q_0 = P_n. \tag{13}$$

2) For C^1 continuity

$$\begin{cases} Q_0 = P_n, \\ Q_1 = P_n + \dfrac{(2n-4)+\pi(1+\alpha_1)-2\omega_1}{(2n-4)+\pi(1+\mu_2)-2\omega_2}(P_n - P_{n-1}). \end{cases} \tag{14}$$

3) For C^2 continuity

$$\begin{cases} Q_0 = P_n, \\ Q_1 = P_n + \dfrac{(2n-4)+\pi(1+\alpha_1)-2\omega_1}{(2n-4)+\pi(1+\mu_2)-2\omega_2}(P_n - P_{n-1}), \\ Q_2 = ([-(2(n-3)+\pi+\dfrac{1}{4}\pi^2(\lambda_1+e^{\omega_1}(1 \\ \quad -\mu_1)))+2(\dfrac{\pi\alpha_1}{2}-\omega_1)-2D]P_{n-2}-(-kn \\ \quad -(n-1)\pi+\dfrac{1}{4}\pi^2\lambda_1-\dfrac{1}{4}\pi^2(\lambda_1+e^{\omega_1}(1-\mu_1)) \\ \quad -(2(n-1)+\pi)(\dfrac{\pi\alpha_1}{2}-\omega_1)+\pi\ \alpha_1\omega_1-\omega_1^2 \\ \quad +2D+2\omega_1-\pi-\pi\alpha_1+2\omega_1-(2n-2))P_{n-1} \\ \quad -[(2(n-2)+\pi)(\dfrac{\pi\alpha_1}{2}-\omega_1)+(2(n-2) \\ \quad +\pi)(-\dfrac{\pi\mu_2}{2}-\omega_2)+(-\dfrac{\pi^2\lambda_1}{4}-\pi\alpha_1\omega_1-\omega_1^2) \\ \quad -(\dfrac{\pi^2\lambda_2}{4}-\pi\mu_2\,\omega_2+\ \omega_2^2)+4k+2\pi+\pi\alpha_1 \\ \quad +\pi\mu_2-2\omega_1-2\,\omega_2]\,P_n+a)b, \end{cases} \tag{15}$$

where,

$$a = \frac{1}{(2(n-2)+\pi(1+\mu_2)-2\omega_2)(d)},$$

$$b = \frac{1}{D_2 - 2D_1 + 2(\omega_2 - \frac{\pi\mu_1}{2})},$$

$$D = \prod_{k\in W}(-k-\frac{\pi}{2}(1+\alpha_1)+\omega_1),$$

$$D_1 = \prod_{k\in W}(k+\frac{\pi}{2}(1+\mu_2)-\omega_2),$$

$$D_2 = -(2n-3)-\pi-\frac{1}{4}\pi^2(e^{\omega_2}(1-\alpha_2)-\lambda_2)$$

$$d = (-kn-(n-1)\pi+\frac{1}{4}\pi^2(\lambda_2-e^{\omega_2}(1 \\ -\alpha_2))-\frac{1}{4}\pi^2)(\lambda_2-2D_1+\pi\ \mu_2\,\omega_2-\omega_2^2 \\ +(2(n-1)+\pi)(\omega_2-\frac{\pi\mu_2}{2})),\quad k\in W.$$

where D and D_1 are the product of series, which are used to generalize the expression of control point Q_2 in C^2 continuity.

Proof:

1) To obtain C^0 continuity condition, we have $H_1(1) = H_2(0)$.
2) For C^1 continuity condition, we solve $H_1(1) = H_2(0)$ and $H_1'(1) = H_2'(0)$ to obtain the results given in equation (14).
3) Similarly, for C^2 continuity condition, we have both C^0 and C^1 continuity conditions. Moreover, we solve $H_1''(1) = H_2''(0)$ for the required control point Q_2 and it yields the result given in equation (15).

Example 1: Figure 3 shows the hybrid trigonometric Bézier curves of degree 3 which satisfy the C^2 continuity conditions at their joints. As described earlier that $\mu_1, \alpha_1, \omega_1, \lambda_1$ and $\mu_2, \alpha_2, \omega_2, \lambda_2$ are the shape parameters of two adjacent curves $H_1(t; \mu_1, \alpha_1, \omega_1, \lambda_1)$ and $H_2(t; \mu_2, \alpha_2, \omega_2, \lambda_2)$, respectively. The control points of $H_1(t; \mu_1, \alpha_1, \omega_1, \lambda_1)$ are $P_0 = (0, 0.2)$, $P_1 = (-0.05, 0.25)$, $P_2 = (0.1, 0.34)$ and $P_3 = (0.2, 0.27)$ while the three control points Q_0, Q_1, Q_2 of $H_2(t; \mu_2, \alpha_2, \omega_2, \lambda_2)$ are obtained by C^2 continuity conditions described in Theorem 3 and last control point of $H_2(t; \mu_2, \alpha_2, \omega_2, \lambda_2)$ is considered according to designer choice.

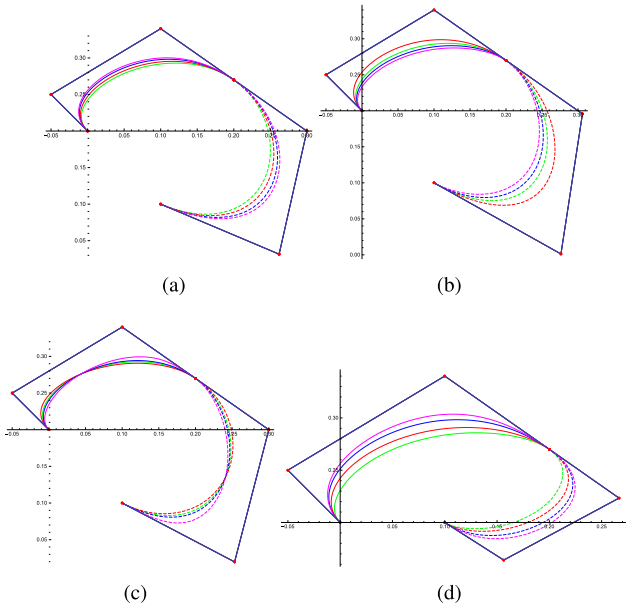

FIGURE 3. C^2 continuity of cubic hybrid trigonometric Bézier curve. **(a):** $\lambda_1 = \lambda_2 = \alpha_1 = \alpha_2 = \omega_1 = \omega_2 = 0, \mu_1 = \mu_2 = 0, 0.37, 0.75, 0.98.$ **(b):** $\lambda_1 = \lambda_2 = \mu_1 = \mu_2 = \omega_1 = \omega_2 = 0, \alpha_1 = \alpha_2 = 0.1, 0.8, -0.4, -1.$ **(c):** $\alpha_1 = \alpha_2 = \mu_1 = \mu_2 = \omega_1 = \omega_2 = 0, \lambda_1 = \lambda_2 = 0, 0.5, -0.5, -1.5.$ **(d):** $\mu_1 = \mu_2 = 0.5, \alpha_1 = \alpha_2 = 1, \omega_1 = \omega_2 = \lambda_1 = \lambda_2 = 0.5, 0.1, -0.2, -0.8.$

Figure 3(a) shows the variation in shape parameters, when we consider $\lambda_1 = \lambda_2 = \alpha_1 = \alpha_2 = \omega_1 = \omega_2 = 0$ and vary the values of $\mu_1 = \mu_2 = 0, 0.37, 0.75, 0.98$. Thin colored lines are obtained by altering the shape parameters of $H_1(t)$ while dotted colored lines are obtained by the variation of shape parameters of $H_2(t)$. In Figure 3(b), the shape of the curve is obtained by keeping the $\lambda_1 = \lambda_2 = \mu_1 = \mu_2 = \omega_1 = \omega_2 = 0$ and varying the values of $\alpha_1 = \alpha_2 = 0.1, 0.8, -0.4, -1$. Similarly, Figure 3(c) shows the variation in graph when keep all other shape parameters fixed to zero and vary the value of $\lambda_1 = \lambda_2 = 0, 0.5, -0.5, -1.5$.

Figure 3(d) is obtained when we keep fixed $\mu_1 = \mu_2 = 0.5$, $\alpha_1 = \alpha_2 = 1$, and vary $\omega_1 = \omega_2 = \lambda_1 = \lambda_2 = 0.5$, 0.1, −0.2, −0.8 simultaneously.

III. SYMMETRIC REVOLUTIONARY CURVES

Let $V = (v_1, v_2, v_3, \ldots, v_n) \in R^n$ be any vector space and $v_1, v_2, v_3, \ldots, v_n$ are their corresponding n vectors. In $2D$ planes two tuples of vector are drawn by using coordinate axis. So, the control points of GHT-Bézier curves are also consist of two tuples of vectors like $P_i = (x_i, y_i)$. But in case of $3D$ planes 3 tuples of vectors like $P_i = (x_i, y_i, z_i)$ are used to construct the surfaces.

In construction of symmetric revolutionary curves about an axis, there are assortment of problem occurs to construct the curves by continuity. So, the key technology to overcome this difficulty is to form an expression by using vectored rational interpolating function. Which will used in graphics and symmetric representation of figures as well.

IV. ALGORITHM FOR THE CONSTRUCTION OF SYMMETRIC REVOLUTIONARY CURVES

The symmetric revolutionary curves can be achieved using following procedure.

1) Given the Bernstein basis functions having the shape parameters $\alpha, \mu, \omega \in [-1, 1]$ and $\lambda \in [-1.5, 0.5]$.
2) Consider the control points $P_i = (x_i, y_i)$, $i = 0, 1, 2, \ldots, n$ in 2D plane.
3) Choose the values of shape parameters α, μ, ω and λ from their given domain.
4) Calculate the functions $x_n(s)$ and $y_n(s)$ by using the definition of GHT-Bézier curve.
5) Put the functions $x_n(s)$ and $y_n(s)$ as xy-coordinates along with the rational factors $\frac{2-s1}{2s1^2-2s1+r}$ and $\frac{-(2-s1)}{2s1^2-2s1+r}$ to obtain $G^x_{symmetricrevolution}$ and $\widetilde{G}^x_{symmetricrevolution}$ or $G^y_{symmetricrevolution}$ and $\widetilde{G}^y_{symmetricrevolution}$ respectively.
6) Plot these both functions and join them to obtain symmetric curves.

Theorem 4: For the set of control points $P_i = (x_i, y_i)$, where $(i = 0, 1, 2, 3, \ldots, n)$, the right revolutionary curve along x-axis is constructed by the control points like $P_i = (x_i, y_i)$ and left revolutionary curve along x-axis is constructed by the control points $P_i = (-x_i, y_i)$ including the rational factors $\frac{2-s}{2\,s^2-2\,s+r}$, where $r \geq 0$ is any positive real number which is used to maximize and minimize the thickness of the desired shape. So, the equation of whole symmetric revolutionary curve along x-axis is obtained by rotating the generating curve $H(t; \mu, \alpha, \omega, \lambda)$ with one revolution is

$$\begin{cases} G^x_{symmetricrevolution}(s, s1; \alpha, \mu, \omega, \lambda) \\ \quad = \left\{ \dfrac{2-s1}{2s1^2-2s1+r} x_n(s), y_n(s) \right\}, \\ \widetilde{G}^x_{symmetricrevolution}(s, s1; \alpha, \mu, \omega, \lambda) \\ \quad = \left\{ -\dfrac{2-s1}{2s1^2-2s1+r} x_n(s), y_n(s) \right\}, \end{cases} \tag{16}$$

where,

$$\begin{cases} x_n(s) = \sum_{i=0}^{n} x_i S_{i,n}(s), \\ y_n(s) = \sum_{i=0}^{n} y_i S_{i,n}(s), \end{cases}$$

and $S_{i,n}(s)$ are GHT-Bernstein basis functions defined by Equation 2. Similarly, upper revolutionary curve along positive y-axis is obtained by the control points $P_i = (x_i, y_i)$ and lower part of the revolutionary curves along negative y-axis is constructed by control points $P_i = (x_i, -y_i)$ including the above mentioned rational factors. So, the equation of whole revolutionary curve along y-axis is

$$\begin{cases} G^y_{symmetric\ revolution}(s, s1; \alpha, \mu, \omega, \lambda) \\ \quad = \left\{ x_n(s), \dfrac{2-s1}{2s1^2-2s1+r} y_n(s) \right\}, \\ \widetilde{G}^y_{symmetric\ revolution}(s, s1; \alpha, \mu, \omega, \lambda) \\ \quad = \left\{ x_n(s), -\dfrac{2-s1}{2s1^2-2s1+r} y_n(s) \right\}. \end{cases} \tag{17}$$

Hence, by splicing above two expressions we can obtain the symmetric revolutionary curves along y-axis.

But straight lines cannot be constructed by using these above expressions. So, by deducting the rational factors from above expressions we can generate the straight lines by using these expressions

$$\begin{cases} G^x_{symmetric}(s; \alpha, \mu, \omega, \lambda) = \{x_n(s), y_n(s)\}, \\ \widetilde{G}^x_{symmetric}(s; \alpha, \mu, \omega, \lambda) = \{-x_n(s), y_n(s)\}, \end{cases} \tag{18}$$

to generate symmetric straight lines along x-axis.

$$\begin{cases} G^y_{symmetric}(s; \alpha, \mu, \omega, \lambda) = \{x_n(s), y_n(s)\}, \\ \widetilde{G}^y_{symmetric}(s; \alpha, \mu, \omega, \lambda) = \{x_n(s), -y_n(s)\}, \end{cases} \tag{19}$$

is used to generate symmetric straight lines along y-axis.

Proof: It is obvious from Definitions 1 and 2.

A. SYMMETRY OF BUTTERFLY BY GHT-BÉZIER REVOLUTIONARY CURVE

The beauty of Mathematics and its balance can often be found in nature. Such type of beauty and structure can be seen in insects, fishes, fruits, planets, shells and clouds etc. This display of structure which is usually found in nature is the motivation for the scholars to study these type of models for their mathematical representation. In such type of natural modeling, examples of mathematical symmetry can be found in number of figures and curves also.

Figure 4 represents a beautiful labeled butterfly (see Figs 4(a) and 4(b)), which is symmetric along y-axis and consists of two upper wings and two lower wings, full body and mouth, antenna, eyes and tail constructed by using GHT-Bézier revolutionary curve with help of Wolfram Mathematica 9 software. Variation in the shape parameters of generating curve which is the dotted wings of the butterfly are constructed by GHT-Bézier curve.

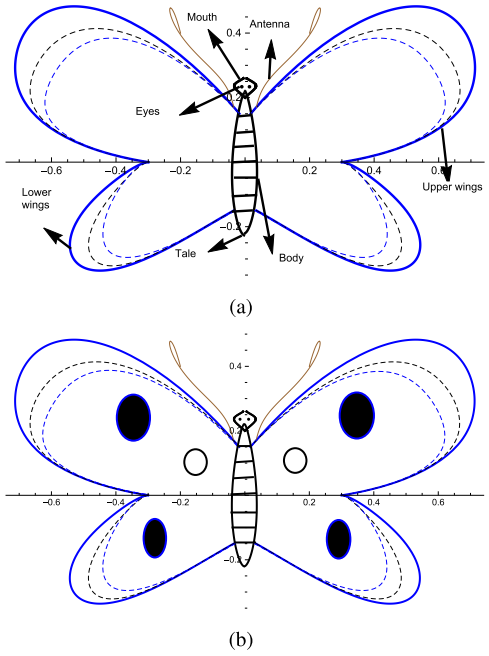

FIGURE 4. Butterfly as the mathematical model of symmetric revolutionary curves. (a): Labeled graph. (b): Beautification of graph.

B. SYMMETRY OF AN APPLE BY GHT-BÉZIER REVOLUTIONARY CURVE

Figure 5 shows the symmetrical representation of an apple along y-axis. The right part of an apple is constructed by using GHT-Bézier revolutionary curve given in Equation 16 with control points $P_i = (x_i, y_i)$ where $x_i = (0, 2.7, 3.3, 2.8, 0)$, $y_i = (2.9, 4.5, 1, -1, -0.5)$, $(i = 0, 1, 2, 3, 4)$. Similarly, the left part is constructed by using the same control points and Equation 16. Figure 5(a) shows the labeled graph of an apple. Figure 5(b) shows the spliced graph which is obtained by joining curves. Thin and dotted lines are obtained by varying the different values of shape parameters. Figure 5(c) shows the beautification in graph by variation of shape parameters.

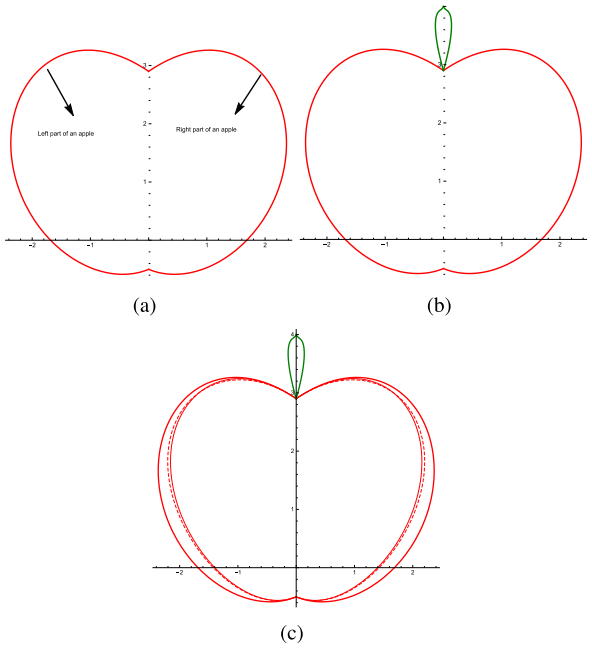

FIGURE 5. Symmetric revolutionary figure of an Apple. (a): Labeled Graph. (b): Spliced Graph. (c): Beautification of graph by variation of shape parameter.

C. SYMMETRY OF A FLOWER BY GHT-BÉZIER REVOLUTIONARY CURVE

Figure 6 shows the symmetrical representation of flower. The two petals of flower are constructed along x-axis shown in Figure 6(a) and two petals are constructed along y-axis shown in Figure 6(b) by equations 16 and 17, respectively. Figure 6(c) shows the connected graph of symmetrical flower. The red and yellow dotted lines are obtained by the variation of shape parameters along x-axis and y-axis.

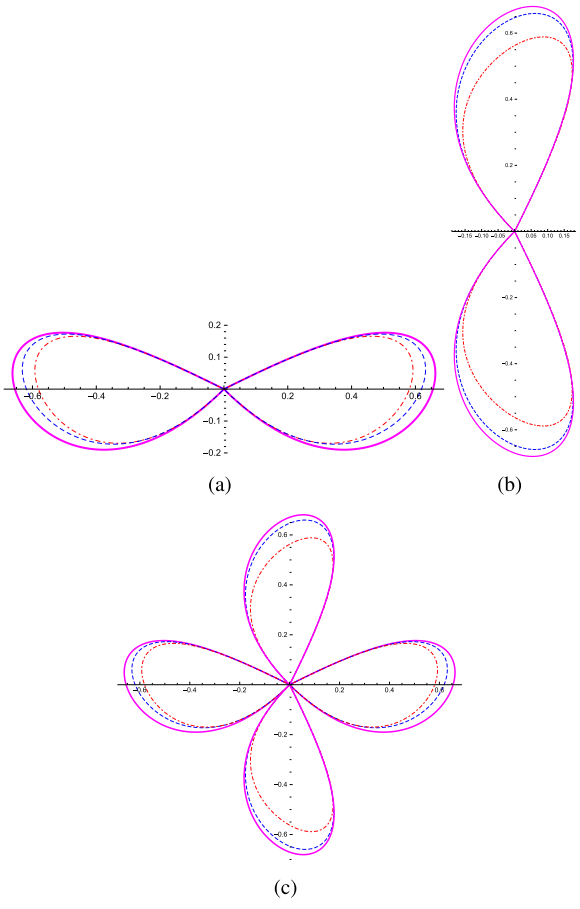

FIGURE 6. Symmetric revolutionary figure of a flower. (a): Symmetry along x-axis. (b): Symmetry along y-axis. (c): Connected graph.

D. SYMMETRY OF A HUT BY GHT-BÉZIER REVOLUTIONARY CURVE

Figure 7 shows the graphical representation of symmetry of Hut along y-axis. This figure is constructed by joining the straight lines. Since above mentioned formulas in equation 16 and 17 are not used to generate the lines due to

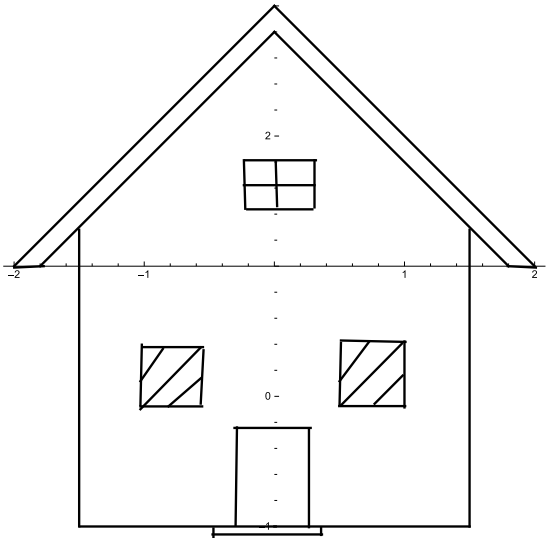

FIGURE 7. Symmetrical representation of Hut.

involving of rational factor. So, after deduction of rational factor the expressions given in equations 18 and 19 are used to construct symmetrical representation of Hut. Figure 7 also shows the efficiency of these curves and CAGD in architectural purpose.

V. CONSTRUCTION OF GHT-BÉZIER SURFACES WITH SHAPE PARAMETERS

Definition 3: For the set of control points $P_{i,j} \in R^3$ where $(i = 0, 1, 2, \ldots, n)$,$(j = 0, 1, 2, \ldots, m)$ and $m, n \geq 3$, the tensor product defined as:

$$R(s, s1; \mu, \alpha, \omega, \lambda, \mu 1, \alpha 1, \omega 1, \lambda 1) = \sum_{i=0}^{n} \sum_{j=0}^{m} P_{i,j} S_{i,n}(s) S_{j,m}(s1), \quad 0 \leq s, s1 \leq 1, \qquad (20)$$

is called GHT-Bézier surface of order m, n with control points $P_{i,j}$. Where $S_{i,n}(s)$ and $S_{j,m}(s1)$ are the GHT-Bernstein basis functions and $\mu, \alpha, \omega, \lambda,$ and $\mu 1, \alpha 1, \omega 1, \lambda 1$ are the shape parameters for the basis functions $S_{i,n}(s)$ and $S_{j,m}(s1)$, respectively.

Remark 1: The tensor product of GHT-Bézier surfaces have the properties similar to the tensor product of classical Bézier surfaces. By keeping the control polygon fixed the shape of the GHT-Bézier surfaces can also be modified by altering the shape parameters. It also possess other properties similar to classical Bèzier surface like angular point interpolation property, symmetry, shape adjustable property, convex hull property, boundary property and affine invariance property.

A. INFLUENCE OF SHAPE PARAMETERS ON GHT-BÉZIER SURFACES

Surfaces are basically generalization of planes. The mutual action of two different curves with the control mesh points in $3D$ planes form surfaces. So, just like curves, surfaces also show the variation in their behaviour by adjustment of different shape parameters.

Example 2: Consider a Bi-cubic hybrid trigonometric Bézier-like surface

$$G(s, s1; \mu, \alpha, \omega, \lambda, \mu^*, \alpha^*, \omega^*, \lambda^*) = \sum_{i=0}^{3} \sum_{j=0}^{3} P_{i,j} S_{i,3}(s) S_{j,3}(s1), \quad 0 \leq s, s1 \leq 1, \qquad (21)$$

with different eight shape parameters $\mu, \alpha, \omega, \lambda$ and $\mu^*, \alpha^*, \omega^*, \lambda^*$ and having sixteen control points. Figure 8 shows the different behaviour of surfaces by the alteration of shape parameters in their domain. Figures 8(a)-8(h) represent the effect of shape parameters when shape is farther away from the control polygon. While by adjustment of these shape parameters, the shape of the surface is moving very close to the control net and its behaviour is shown in the Figs 8(f)-8(h).

B. GHT-BÉZIER SYMMETRIC ROTATION SURFACES

Just like revolution surfaces, the problem of rotation surfaces about an arbitrary axis in three dimensions plays a vital role in many fields including molecular simulation, architectural design and computer graphics etc. A rotation surface is generated by rotating a two dimensional curve about an axis of rotation in space, the resulting surface therefore has an azimuthal symmetry. In $3D$, if we translate a space the rotation axis passes through the origin. If we rotate a space about the z-axis then rotation axis lies in xoz plane and by rotating the space about y-axis, the rotation axis lies along the z-axis. Hence, by making use of basic translational transformation and rotation transformation, the GHT-Bézier symmetric rotation surfaces can be moved in any orientation to the specified location.

For any surface, the axis of rotation in the space is shown in the Figure 9 [24].

Consider a GHT-Bézier curve as a generating line in the plane xoy. If the axis of rotation is x-axis for generating symmetric surfaces, then the matrix representation and equation of rotation can be expressed as:

$$X_{Symmetric-rotation} = \begin{bmatrix} 1 & 0 & 0 \\ 0 & cos(s1) & -sin(s1) \\ 0 & sin(s1) & cos(s1) \end{bmatrix} H(s) = [x(s), y(s)cos(s1), y(s)sin(s1)]^T. \qquad (22)$$

Similarly for yoz plane and xoz plane, the equation of rotation surface for y-axis and z-axis can be expressed as:

$$Y_{Symmetric-rotation} = \begin{bmatrix} cos(s1) & 0 & sin(s1) \\ 0 & 1 & 0 \\ -sin(s1) & 0 & cos(s1) \end{bmatrix} H(s) = [z(s)cos(s1), y(s), z(s)sin(s1)]^T, \qquad (23)$$

$$Z_{Symmetric-rotation} = \begin{bmatrix} cos(s1) & -sin(s1) & 0 \\ sin(s1) & cos(s1) & 0 \\ 0 & 0 & 1 \end{bmatrix} H(s) = [x(s)cos(s1), x(s)sin(s1), z(s)]^T, \qquad (24)$$

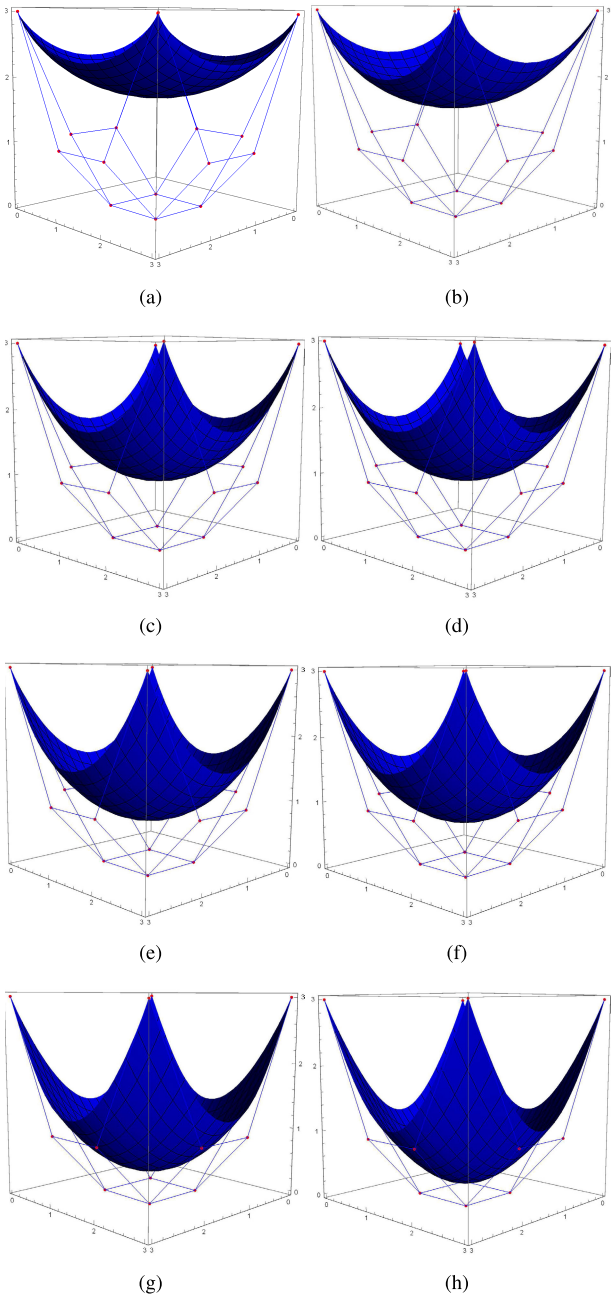

FIGURE 8. Bi-cubic hybrid trigonometric Bézier surfaces with different shape parameters. (a): (−0.5, −0.5, 1, 0.5, −0.5, −0.5, 1, 0.5). (b): (−0.75, 0.75, −0.75, −0.25, 0.9, −0.25, 0.9, 0.5). (c): (−1, −0.5, −1, −0.5, −1, −0.5, −1, −0.5). (d): (0.9, −0.25, 0.9, −0.25, 0.9, −0.25, 0.9, −0.25). (e): (0.9, 0.8, 1, 0.5, 0.9, 0.8, 1, 0.5). (f): (0, 0, 0, 0, 0, 0, 0, 0). (g): (0.9, 0.8, 1, 0.5, 0.9, 0.8, 1, 0.5). (h): (1, 0, 1, 0, 1, 0, 1, 0).

where $0 \leq s1 \leq 2\pi$. So, by using GHT-Bézier curve as a generating curve, we can construct a family of rotation surfaces and can modify the shape of the figures according to our own choice by adjusting the values of shape parameters.

Theorem 5: For the given coordinates $(0, y_i, z_i)$ of the control points P_i where $(i = 0, 1, 2, \ldots, n)$ in yoz plane, the equation of whole rotation surface is obtained by rotating the generating curve $H(s; \alpha, \mu, \omega, \lambda)$ around y-axis with one

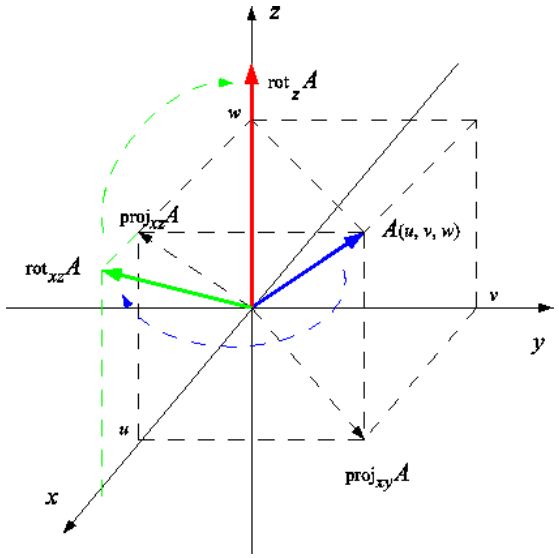

FIGURE 9. Rotation about arbitrary axis in 3*D*.

revolution is

$$\begin{cases} Y_{symmetric-rotation}(s, s1; \alpha, \mu, \omega, \lambda) \\ \quad = \left\{ \dfrac{1 - 2s1}{2s1^2 - 2s1 + 1} z_n(s), y_n(s), \dfrac{2s1 - 2s1^2}{2s1^2 - 2s1 + 1} z_n(s) \right\}, \\ \widetilde{Y}_{symmetric-rotation}(s, s1; \alpha, \mu, \omega, \lambda) \\ \quad = \left\{ \dfrac{-(1 - 2s1)}{2s1^2 - 2s1 + 1} z_n(s), y_n(s), \dfrac{-(2s1 - 2s1^2)}{2s1^2 - 2s1 + 1} z_n(s) \right\}, \end{cases} \tag{25}$$

and by joining these two expressions $Y_{symmetric-rotation}$ and $\widetilde{Y}_{symmetric-rotation}$, we can obtained the GHT-Bézier rotation surface in yoz plane. The components $y_n(s)$ and $z_n(s)$ are given as:

$$\begin{cases} y_n(s) = \sum_{i=0}^{n} y_i S_{i,n}(t), \\ z_n(s) = \sum_{i=0}^{n} z_i S_{i,n}(t), \end{cases} \tag{26}$$

where $S_{i,n}(t)$ are the GHT-Bernstein basis functions, y_i and z_i are the coordinates of the control points.

Proof: The proof is given in [11].

Similarly, the symmetric rotation surfaces in xoy and xoz can also be generated by rotation formula.

C. SYMMETRY OF A CHALICE BY GHT-BÉZIER ROTATION SURFACE

In practical applications, the designers mostly starts with a rough idea to make the required shape of surface. They usually made an algorithm to compute their idea to display the result. A common example is a rotation surface. Figure 10(a) and Figure 10(b) represent the left and right part of symmetry, respectively. Figure 10 shows the connected graph of Chalice by using GHT-Bézier rotation surface see Theorem 5. Figures 11(a)-11(f) show the symmetric representation of Chalice surfaces by GHT-Bézier rotation surface with different shape parameters. Due to the fact that, the rotation surface possess four different shape parameters, by varying

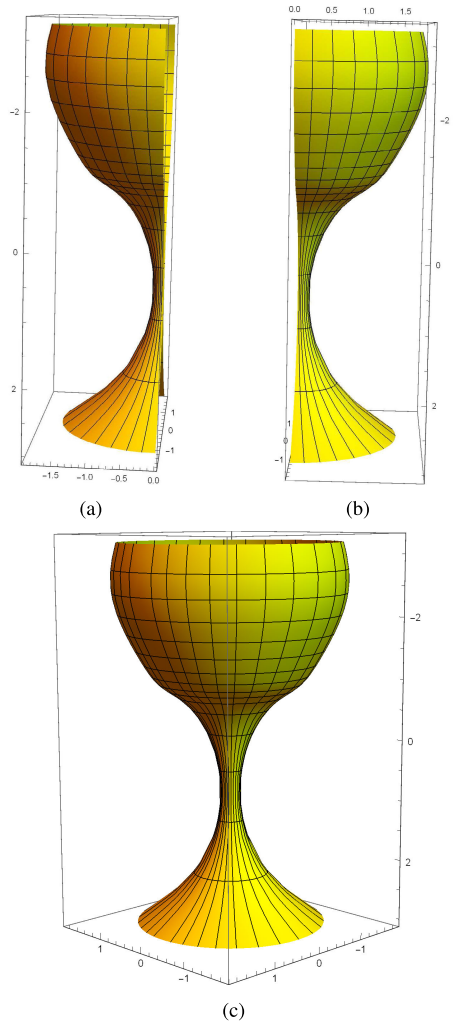

FIGURE 10. Construction of symmetric Figure of Chalice. (a): Left portion of symmetry. (b): Right portion of symmetry. (c): Connected of graph of Chalice.

these shape parameters we can modify the shape of the curve according to our own choice. For the set of control points $P_i(i = 0, 1, 2, 3, \ldots, 11)$ in xoy plane, whose coordinates are taken as:

$$\begin{cases} P_0=(-3.2, 1.8, 0), & P_1=(-2.5, 2, 0), \ P_2=(-2, 2, 0), \\ P_3=(-1.5, 1.5, 0), & P_4=(-1, 1, 0), \ P_5=(-0.7, 1.1, 0), \\ P_6=(-0.7, 1, 0), & P_7=(-0.6, 1.2, 0), \ P_8=(-1.5, 0, 0), \\ P_9=(1.5, -0.4, 0), & P_{10}=(2, 0.1, 0), \ P_{11}=(3, 1.54, 0). \end{cases}$$

By using expressions given in Theorem 5, we can obtain the symmetric representation of chalice as shown in Figure 11.

D. SYMMETRY OF A CERAMIC POT BY GHT-BÉZIER ROTATION SURFACES

Figure 12 shows the symmetric representation of Ceramic Pots in xoz plane by GHT-Bézier rotation surface with variation of different shape parameters. These figures are symmetric about z-axis. Width of these surfaces can be altered by adjusting the different values of different shape parameters for the required shape.

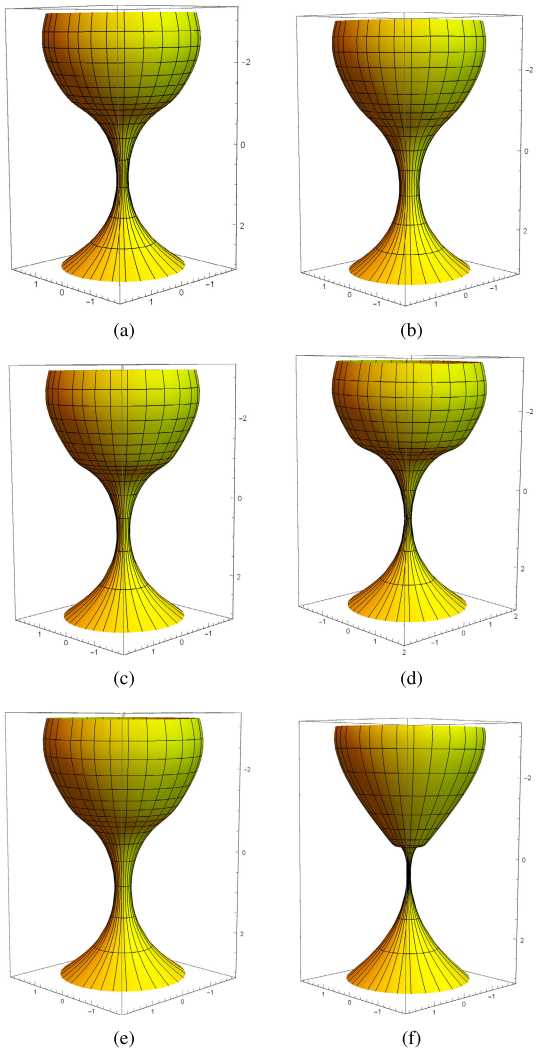

FIGURE 11. Representation of Chalice as a GHT-Bézier symmetric rotation surface with different values of shape parameters. (a): $(\alpha, \mu, \omega, \lambda) = (0, 0, -1, 0)$. (b): $(0, 1, 1, 0)$. (c): $(-1, 0, 0, 0.5)$. (d): $(0.8, 0.8, 1, 0.5)$. (e): $(1, 1, 1, 0.5)$. (f): $(0.9, 0.9, 1, 0.5)$.

E. SYMMETRY OF A CAPSULE TORUS BY GHT-BÉZIER ROTATION SURFACES

Figure 13 shows the symmetric representation of Capsule Torus which also act as a rotation surface and it can rotate about an axis of rotation. As the distance of the Torus surface from the axis of rotation is decreases, its width also decreases but by increasing the distance between the axis of rotation and Torus surface, its width become increases. Since the GHT-Bézier rotation surface possess four different shape parameters and by variation of these shape parameters, we can see alteration in the surface of Capsule Torus. This Capsule Torus which is made by GHT-Bézier rotation surface technique has smooth shape on both surfaces but as we varies the values of its shape parameters, the surface altered.

VI. ALGORITHM OF DESIGNING SYMMETRIC ROTATION SURFACES

The symmetric rotation surfaces can be designed by using following algorithm.

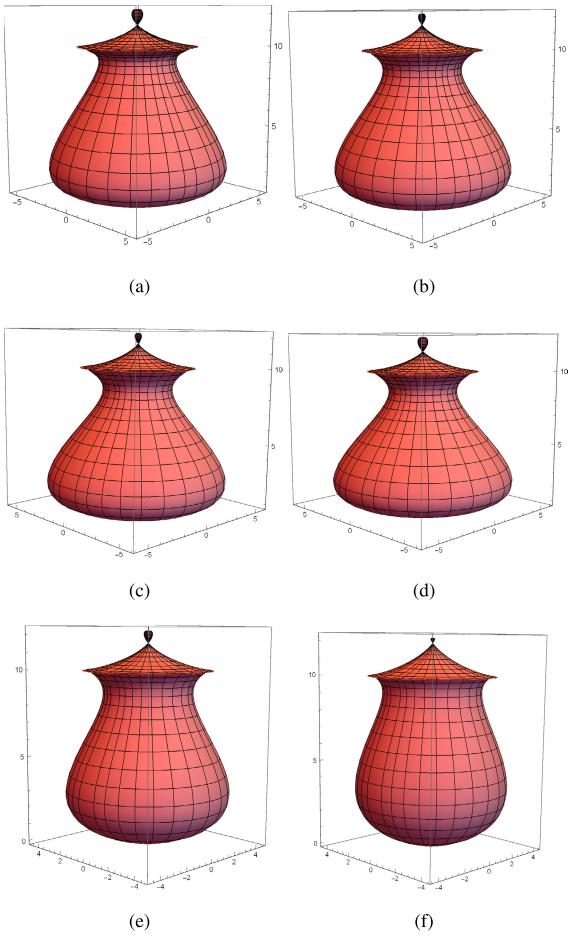

FIGURE 12. Representation of Ceramic Pot as a GHT-Bézier rotation surface with different values of shape parameters. (a): $(\alpha, \mu, \omega, \lambda) = (0, 1, 0, 0)$. (b): (0, 0, 1, 0.5). (c): (−1, −1, 0, 0). (d): (0, 0, 0, 0.5). (e): (1, 1, 1, 0.5). (f): (1, 0, 0, 0).

1) Given GHT-Bernstein basis functions having the shape parameters $\alpha, \mu, \omega \in [-1, 1]$ and $\lambda \in [-1.5, 0.5]$.
2) Suppose we want to construct any symmetric rotation surface in *yoz* plane.
3) Consider these control points $P_i = (0, y_i, z_i)$, $i = 0, 1, 2, \ldots, n$ in 3D plane.
4) Choose the shape parameters α, μ, ω and λ from their given domain.
5) Calculate the functions $y_n(s)$ and $z_n(s)$ by using the definition of GHT-Bézier curve.
6) Put the functions $x_n(s)$ and $z_n(s)$ as coordinates in 3D plane along with their rational factors which are $\frac{1-2s1}{2s1^2-2s1+1}$ and $\frac{2s1-2s1^2}{2s1^2-2s1+1}$ to construct $Y_{Symmetric-rotation}$ and use $\frac{-(1-2s1)}{2s1^2-2s1+1}$ and $\frac{-(2s1-2s1^2)}{2s1^2-2s1+1}$ to construct $\widetilde{Y}_{Symmetric-rotation}$ to form the symmetric rotation surfaces.
7) Plot these two functions and join them to obtain symmetric figures in *yoz* plane.

Similarly, the symmetric rotation surfaces can also be constructed in *xoy* plane and *xoz* plane by interchanging the coordinates.

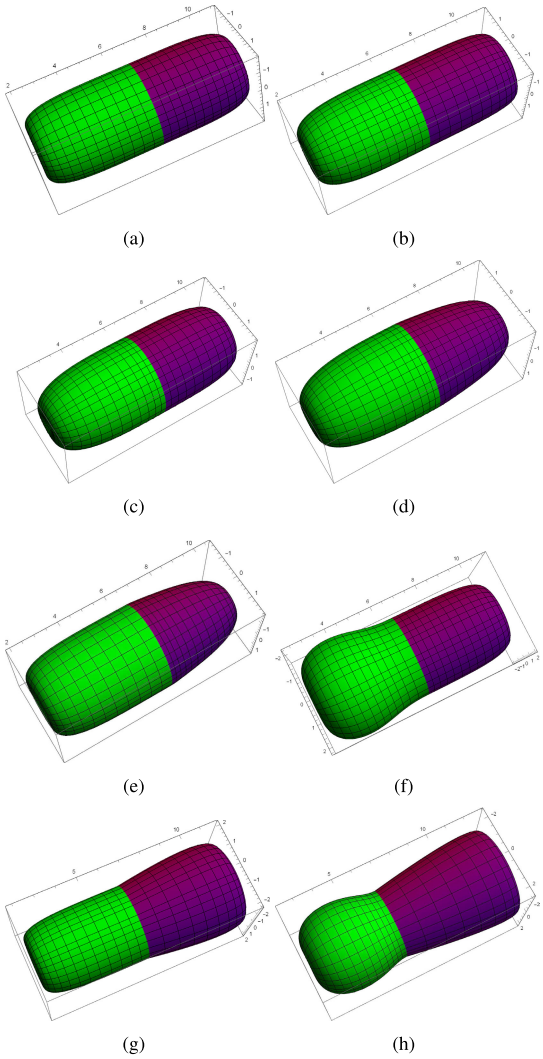

FIGURE 13. Symmetric GHT-Bézier rotation surfaces of capsule torus with different values of shape parameters. (a): (0,0,0,0,0,0,0,0). (b): (0.5, 0, 0, 0, 0.5, 0, 0, 0). (c): (−0.5, −1, 0.5, 1, −0.5, −1, 0.5, 1). (d): (−0.5, −1, 1, 0.5, −1, −1, −1, −1). (e): (−1, 0.5, 0.5, 0.5, −1, −1, −1, 0.5). (f): (−0.5, 1, 1, 0.5, −0.5, 1, 1, 0.5). (g): (−1, −1, −1, −1.5, −1, −1, −1, −1.5). (h): (−1, −1, −1.5, 0, −1, −1, −1.5, 0).

VII. APPLICATIONS OF SYMMETRIC FIGURES

In industrial production, we should consider these two main formulas (given in this study) if the product of symmetric curves and surfaces (such as in buildings, aircraft wings, sketches of butterfly, flowers, ceramic pots etc.) cannot be designed easily by joining Bézier curve and Bézier surface by continuity conditions. By using the method described in this paper various kinds of symmetric revolutionary curves and symmetric rotation surfaces with multiple shape parameters have been constructed flexibly.

Roughly speaking, this study is time saving for us because any symmetric figure can be drawn easily in one stroke by using this method while by using simple continuity conditions it will take twice time. Furthermore, the construction of symmetric figures are helpful in mathematics, architectural, industry and engineering purposes. Some figures are

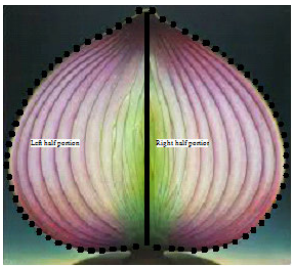

(a) Symmetrical effect of GHT-Bézier curve in nature

(b) Symmetry in nature

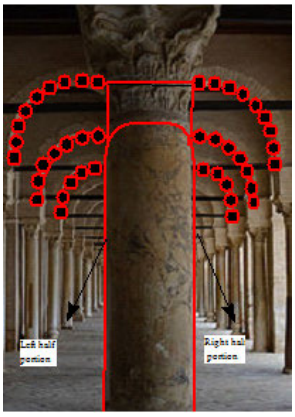

(c) Symmetrical effect of GHT-Bézier curve civil engineering

(d) Symmetry in civil engineering

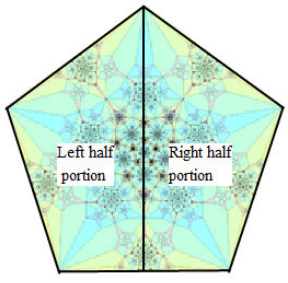

(e) Symmetrical effect of GHT-Bézier curve in Fractals (Mathematics)

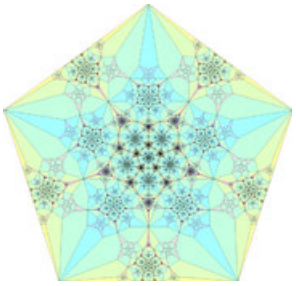

(f) Symmetry in Fractals (Mathematics)

FIGURE 14. Real life applications of symmetry curves with different shape parameters (a): (1, 1, 1, 1). (c): (0.5, 0, 0, 0, 0.5). (e): (0.5, 1, 0, 0.5). (a) Symmetry in nature. (b) Symmetry in civil engineering. (c) Symmetry in Fractals (Mathematics).

given here which shows the representation of symmetry along y-axis can be constructed by the method given in this paper. Because when we divide or fold into half so that the two halves match exactly.

Just like, Figure 14 shows the application of symmetrical representation in engineering/industrial field and in natural life. Figure 14(c) and 14(d) is the best example of civil/architectural engineering because here we need to construct only one portion (right/left portion) of this building while the second portion will be obtained automatically by using the formulas given in above literature. Similarly, other two figures can also be drawn by using the above algorithm.

VIII. CONCLUSION

In this paper, we have constructed GHT-Bernstein basis functions with four different shape parameters, studied their properties and also presented their shapes of multiple degrees. By using these GHT-Bernstein basis functions, we have constructed GHT-Bézier curves and also presented their parametric continuity. Then we extended these GHT-Bézier curves up to tensor product surfaces. The influence of shape parameters on surfaces is also presented here. The dominant analysis of this paper is the construction of symmetric revolutionary curves and symmetric rotation surfaces by using specific formulas. Based on these GHT-Bézier curves and formulas, the symmetric Figures of Butterfly, Apple, Flower, Hut, Chalice, Ceramic Pot and Capsule Torus is presented. The variation in Figures with the shape parameters is also presented. Finally, use of this literature in natural life and applications of this literature is also given here. In short, construction of any type of symmetric curves and symmetric rotation surfaces with these formula is very effective, significant and time saving process.

REFERENCES

[1] L. Xikun, "Bernstein-Bézier class curves and a reparametrization method of Bézier curve," *J. Comput. Res. Develop.*, vol. 41, no. 6, pp. 1016–1021, 2004.
[2] L. Yan and J. Liang, "An extension of the Bézier model," *Appl. Math. Comput.*, vol. 218, no. 6, pp. 2863–2879, 2011.
[3] G. Farin, *Curves and Surfaces for CAGD: A Practical Guide*. New York, NY, USA: Academic, 2002.
[4] X. J. Li, H. Liu, G. He, and W. Liao, "Generation and shape adjustment of revolution surface based on stream curve," *Mech. Sci. Technol.*, vol. 27, no. 3, pp. 326–329, 2008.
[5] H. Liu, L. Li, D. Zhang, and H. Wang, "Cubic trigonometric polynomial B-spline curves and surfaces with shape parameter," *J. Inf. Comput. Sci.*, vol. 9, no. 4, pp. 989–996, 2012.
[6] J. Li, "A novel Bézier curve with a shape parameter of the same degree," *Results Math.*, vol. 73, pp. 159–170, Dec. 2018.
[7] W. Wen-Tao and W. Guo-Zhao, "Bézier curves with shape parameter," *J. Zhejiang Univ.-Sci. A*, vol. 6, no. 6, pp. 497–501, 2004.
[8] G. Hu, H. Cao, S. Zhang, and G. Wei, "Developable Bézier-like surfaces with multiple shape parameters and its continuity conditions," *Appl. Math. Model.*, vol. 45, pp. 728–747, May 2017.
[9] X.-A. Han, Y. Ma, and X. Huang, "The cubic trigonometric Bézier curve with two shape parameters," *Appl. Math. Lett.*, vol. 22, pp. 226–231, Feb. 2009.
[10] C. L. Dai, Y. L. Ding, and X. Lu, "On generalized revolving surface based on metamorphose curve," *Mech. Sci. Technol.*, vol. 21, no. 4, pp. 537–539, 2002.
[11] G. Hu, G. Wei, and J. Wu, "Shape Adjustable Generalized Bézier Rotation with the multiple shape parameters," *Results Math.*, vol. 72, pp. 1281–1313, Nov. 2017.
[12] G. Hu, J. Wu, and X. Qin, "A novel extension of the Bézier model and its applications to surface modeling," *Adv. Eng. Softw.*, vol. 125, pp. 27–54, Nov. 2018.
[13] G. Hu, C. Bo, J. Wu, G. Wei, and F. Hou, "Modeling of free-form complex curves using SG-Bézier curves with constraints of geometric continuities," *Symmetry*, vol. 10, no. 11, pp. 545–567, 2018.
[14] G. Hu, H. Cao, X. Qin, and X. Wang, "Geometric design and continuity conditions of developable λ-Bézier surfaces," *Adv. Eng. Softw.*, vol. 114, pp. 235–245, Dec. 2017.
[15] X. Qin, G. Hu, N. Zhang, X. Shen, and Y. Yang, "A novel extension to the polynomial basis functions describing Bézier curves and surfaces of degree n with multiple shape parameters," *Appl. Math. Comput.*, vol. 223, pp. 1–16, Oct. 2013.
[16] M. Dube and R. Sharma, "Quartic trignometric Bézier curve with a shape parameter," *Int. J. Math. Comput. Appl. Res.*, vol. 3, no. 3, pp. 89–96, 2013.

[17] X. Qin, X. Shen, G. Hu, "Shape modification for quartic C-Bézier curves," *Comput. Eng. Appl.*, vol. 50, no. 13, pp. 178–181, 2014.
[18] R. Sharma and M. Dube, "Shape features of cubic trigonometric Bézier curve with two shape parameters," in *Proc. Nat. Conf. Pure Appl. Math.*, 2015, pp. 13–17.
[19] Y. Zhu, X. Han, and J. Han, "Quartic trigonometric Bézier curves and shape preserving interpolation curves," *J. Comput. Inf. Syst.*, vol. 8, no. 2, pp. 905–914, 2012.
[20] X. Qin, G. Hu, Y. Yang, and G. Wei, "Construction of PH splines based on H-Bézier curves," *Appl. Math. Comput.*, vol. 238, pp. 460–467, Jul. 2014.
[21] U. Bashir, M. Abbas, and J. M. Ali, "The G^2 and C^2 rational quadratic trigonometric Bézier curve with two shape parameters with applications," *Appl. Math. Comput.*, vol. 219, pp. 10183–10197, Jun. 2013.
[22] X. Han, "Piecewise quadratic trigonometric polynomial curves," *Math. Comput.*, vol. 72, no. 243, pp. 1369–1378, 2003.
[23] H. Y. Geum and I. Y. Kim, "On the analysis and construction of the butterfly curve using Mathematica," *Int. J. Math. Educ. Sci. Technol.*, vol. 39, no. 5, pp. 670–678, 2006.
[24] M. Glenn, *Rotation About an Arbitrary Axis in 3 Dimensions*. Mountain View, CA, USA: Google, 2013.
[25] M. Y. Misro, A. Ramli, and J. M. Ali, "S-shaped and C-shaped transition curve using cubic trigonometric Bézier," *Amer. Inst. Phys.*, vol. 41, no. 6, pp. 1016–1021, 2017.
[26] M. Y. Misro, A. Ramli, and J. M. Ali, "Quintic trigonometric Bézier curve and its maximum speed estimation on highway designs," in *Proc. AIP Conf.*, 2018, Art. no. 020089.
[27] L. Yan, "Adjustable Bézier curves with simple geometric continuity conditions," *Math. Comput. Appl.*, vol. 21, no. 44, p. 44, 2016.
[28] G. Hu, J. Wu, and X. Qin, "A new approach in designing of local controlled developable H-Bézier surfaces," *Adv. Eng. Softw.*, vol. 121, pp. 26–38, Jul. 2018.
[29] R. Sharma, "A class of QT Bézier curve with two shape parameters," *Int. J. Sci. Res.*, vol. 5, no. 5, pp. 131–134, 2016.
[30] F. Liu, X. Ji, G. Hu, and J. Gao, "A novel shape-adjustable surface and its applications in car design," *Appl. Sci.*, vol. 9, no. 11, p. 2339, 2019.
[31] C. Fu, M. Uddin, and A. C. Robinson, "Turbulence modeling effects on the CFD predictions of flow over a NASCAR Gen 6 racecar," *J. Wind Eng. Ind. Aerodyn.*, vol. 176, pp. 98–111, May 2018.
[32] H. Chowdhury, R. Islam, M. Hussein, M. Zaid, B. Loganathan, and F. Alam, "Design of an energy efficient car by biomimicry of a boxfish," *Energy Proc.*, vol. 160, pp. 40–44, Feb. 2019.
[33] M.-C. Hsu, C. Wang, F. Xu, A. J. Herrema, and A. Krishnamurthy, "Direct immersogeometric fluid flow analysis using B-rep CAD models," *Comput. Aided Geometric Des.*, vol. 43, pp. 143–158, Mar. 2016.
[34] B. Kumar and P. Sarkar, "Prediction of future car forms based on historical trends," *Perspect. Sci.*, vol. 8, pp. 764–766, Sep. 2016.
[35] E. Ostrosi, J.-B. Bluntzer, Z. Zhang, and J. Stjepandic, "Car style-holon recognition in computer-aided design," *J. Comput. Des. Eng.*, vol. 6, pp. 719–738, Oct. 2018.
[36] J. Guo, F. Ding, X. Jia, and D.-M. Yan, "Automatic and high-quality surface mesh generation for CAD models," *Comput.-Aided Des.*, vol. 109, pp. 49–59, Apr. 2019.
[37] Y. Xiong, Y. Li, P. Y. Pan, and Y. A. Chen, "A regression-based Kansei engineering system based on form feature lines for product form design," *Adv. Mech. Eng.*, vol. 8, no. 7, pp. 1–12, Jul. 2016.
[38] F. Pei, X. L. Han, and Y. Li, "Structure and splice of Coons patched with shape parameters," *Comput. Eng. Appl.*, vol. 49, no. 10, pp. 163–166, 2013.
[39] W. Shen and G. Wang, "Geometric shapes of C-Bézier curves," *Comput.-Aided Des.*, vol. 58, pp. 242–247, Jan. 2015.
[40] D. E. Aljure, J. Calafell, A. Baez, and A. Oliva, "Flow over a realistic car model: Wall modeled large eddy simulations assessment and unsteady effects," *J. Wind Eng. Ind. Aerodyn.*, vol. 174, pp. 225–240, Mar. 2018.
[41] H. Cao, G. Hu, G. Wei, and S. Zhang, "Offset approximation of hybrid hyperbolic polynomial curves," *Results Math.*, vol. 72, no. 12, pp. 1055–1071, 2017.
[42] R. Lee and Y. J. Ahn, "Limit curve of H-Bézier curves and rational Bézier curves in standard form with the same weight," *J. Comput. Appl. Math*, vol. 281, pp. 1–9, Jun. 2015.
[43] B. Jüttler and M. L. Sampoli, "Hermite interpolation by piecewise polynomial surfaces with rational offsets," *Comput. Aided Geometric Des.*, vol. 17, no. 4, pp. 361–385, 2000.
[44] T. Maekawa and J. Chalfant, "Design and tessellation of B-spline developable surfaces," *Comput. Aided Geometric Des.*, vol. 120, no. 3, pp. 453–461, 1998.

SAMIA BIBI was born in Pakistan, in October 1994. She received the B.S. (Hons.) and M.Phil. degrees in mathematics from the University of Sargodha, Sargodha, Pakistan, in 2016 and 2018, respectively. She has been a Visiting Lecturer with the University of Sargodha, since 2016. She taught various courses in applied mathematics. Her research interests include mathematical modeling, curve approximation, and CAGD.

MUHAMMAD ABBAS was born in Pakistan, in August 1979. He received the B.Sc. and M.Sc. degrees from the University of the Punjab, Lahore, Pakistan, in 2001 and 2003, respectively, and the Ph.D. degree in computer aided geometric design from the School of Mathematical Sciences, Universiti Sains Malaysia, Penang, Malaysia, in 2012. He completed a postdoctoral fellowship, in 2014. He started his career as a Lecturer with the University of Sargodha, Sargodha, Pakistan, in 2005. He taught a variety of courses in applied mathematics for the bachelor's and master's degree level students. He is an Associate Professor of computational and applied mathematics with the University of Sargodha. He has published many research articles in peer-reviewed impact factor journals and international conferences, in his area of research. His research interests include the development of the shape-preserving scientific data visualization schemes, geometric modeling, and numerical solution techniques for PDEs, ODEs, FPDEs, and FODEs using B-spline functions.

MD YUSHALIFY MISRO received the B.Sc. and M.Sc. degrees (Hons.) in mathematics and the Ph.D. degree in computer aided geometric design from Universiti Sains Malaysia (USM), in 2017. He joined the School of Mathematical Sciences, USM, in 2018. His research interests include the areas of trigonometric Bézier curves, road/railway design, curvature continuous path planning, and transportation. He has published numerous publications in indexed journals and conference proceedings. He is a member of the Malaysian Mathematical Sciences Society (PERSAMA). He has reviewed several academic journals such as the *Malaysian Journal of Mathematical Sciences*. He has also reviewed International Conference Proceedings by the ACM.

GANG HU was born in China, in April 1979. He received the master's degree in applied mathematics from Northwestern Polytechnical University and the Ph.D. degree in mechanical engineering from the Xi'an University of Technology, Xi'an, China. He is currently a Professor of computer engineering and applied mathematics with the Xi'an University of Technology. He started his career as a Lecturer with the Xi'an University of Technology, in 2002, and taught a variety of courses in applied mathematics for master's and bachelor's degree students. His work has been published in a number of different journals. His research interests include computation geometry, CAD/CAM, computer graphics, image processing, and applied mathematics. He is a member of the Chinese Computer Federation and a member of the CSIAM. He has served as a program committee member of numerous international conferences.